A&A 463, 393–397 (2007)
DOI: 10.1051/0004-6361:20065906

Astronomy & Astrophysics

The constancy of the Pioneer anomalous acceleration

Ø. Olsen

Institute of Theoretical Astrophysics, University of Oslo, PO Box 1029 Blindern, 0315 Oslo, Norway
e-mail: oystein.olsen@astro.uio.no

Received 26 June 2006 / Accepted 8 November 2006

ABSTRACT

Aims. The temporal evolution of the Pioneer anomalous acceleration is studied to determine its correlation with solar activity.
Methods. Bayesian Weighted Least Squares algorithms and Kalman filters are used to study the temporal evolution of the Pioneer anomalous acceleration. Doppler data for Pioneer 10 and 11 spanning respectively 11 and 3.5 years were used in this study.
Results. The Doppler data itself can not be used to distinguish between a constant acceleration model and acceleration proportional to the remaining plutonium in the radioisotope thermoelectric generators. There are significant short term variations in the anomalous acceleration. These are shown to be consistent with radio plasma delay from coronal mass ejections.

Key words. celestial mechanics – ephemerides

1. Introduction

The Pioneer 10 and 11 missions were the two first spacecraft to explore the outer Solar System. Anderson et al. (2002)[1] found a small unmodeled acceleration acting on the spacecraft. The magnitude of the acceleration is approximately 8×10^{-8} cm/s^2 with a direction towards the inner Solar System. Explanations of this anomaly range from the new physics to overlooked conventional forces. Scheffer (2003) argues for non-isotropic radiation of spacecraft heat as the most likely candidate. In this Paper I study the temporal variations of the anomalous acceleration to see if any model can be excluded.

PA together with its references provide comprehensive descriptions of the Pioneer spacecraft and the Deep Space Network (DSN) communications system. This will not be repeated in this paper.

2. Analysis of the data

Moyer (2000) provides the formulation for observed and computed values of DSN data types for navigation. Only a cursory description for doppler data is provided in this paper as the Orbit Data File (ODF) tracking data consists of time series of observed doppler counts, which can be converted to time series of doppler frequencies with given count intervals, T_C.

Moyer designates the transmission time from Earth as t_1, the epoch of retransmission as t_2 and the reception time as t_3. At each of these epochs the Solar System Barycentric (SSB) position of the uplink station $\boldsymbol{r}_1$, spacecraft $\boldsymbol{r}_2$ and downlink station $\boldsymbol{r}_3$ must be calculated. The range r_{ij} is defined as the magnitude of the vector $\boldsymbol{r}_j - \boldsymbol{r}_i$. Computed values for two-way and three-way doppler observables are then found from

$$F_{2,3} = \frac{M_{2R}}{T_C}\int_{t_{3s}}^{t_{3e}} f_T(t_3)\mathrm{d}t_3 - \frac{M_2}{T_C}\int_{t_{1s}}^{t_{1e}} f_T(t_1)\mathrm{d}t_1, \quad (1)$$

where $M_{2R} = M_2 = 240/221$ for S-band communication. $f_T(t_3)$ and $f_T(t_1)$ are the transmitter frequencies at reception and transmission time at the receiving and transmitting electronics. The integration limits t_{3s} and t_{3e} are the beginning and end of each count interval at the receiving station, while t_{1s} and t_{1e} are the start and end times of the corresponding interval at the uplink station. t_{1s} and t_{1e} can be found from t_{3s} and t_{3e} and the precision round-trip light time solutions ρ_e and ρ_s. The precision round-trip light times were computed from

$$\begin{aligned}\rho &= \frac{r_{23}}{c} + RLT_{23} + \frac{r_{12}}{c} + RLT_{12} \\ &\quad -\Delta T_{t3} - \Delta T_{t1} \\ &\quad +\frac{1}{c}\Big(\Delta_A\rho(t_3) + \Delta_{SC}\rho_{23} + \Delta_A\rho(t_1) + \Delta_{SC}\rho_{12}\Big), \end{aligned} \quad (2)$$

where RLT_{ij} is the Shapiro delay on the upleg and downleg light time solutions. r_{23} is the distance between receiver at reception time and the spacecraft at retransmission time. Similarily, r_{12} is the distance between transmitter at transmission time and the spacecraft at retransmission time. c is the speed of light. $\Delta_A\rho(t_i)$ are the off-axis antenna corrections to the receiving and transmitting station on Earth. The values used to calculate these corrections where taken from Imbriale (2002). $\Delta_{SC}\rho_3$ and $\Delta_{SC}\rho_1$ are the solar corona corrections on the down and up leg. The Cassini model was used for this study, but as pointed out by PA, the net effect of the solar corona is small and can ultimately be ignored. The model itself is given by PA. ΔT_3 and ΔT_1 are the differences between Coordinated Universal Time (UTC) and Barycentric Dynamical Time (TDB) at transmission and reception time.

Troposphere and ionosphere corrections were not included in the light time solution, but added as a media correction to the Doppler observable. Media corrections for two-way and three-way computed Doppler observables are given by

$$\Delta F_{2,3} = \frac{M_2}{T_C}\left(f_T(t_{1e})\Delta\rho_e - f_T(t_{1s})\Delta\rho_s\right). \quad (3)$$

$\Delta\rho_e$ and $\Delta\rho_s$ are the correction to the precision round-trip light times at the end and beginning of the transmission interval. The frequencies at the start and end of the transmission interval must

[1] Herafter denoted as PA.

be known. Media corrections are computed both for the up-leg and down-leg part of the light time solution.

Finally, partials of the computed Doppler observables with respect to solve-for parameters $\boldsymbol{q}$ are required:

$$\frac{\partial F_{2,3}}{\partial \boldsymbol{q}} = \frac{M_2}{T_C}\left(f_T(t_{1e})\frac{\partial \rho_e}{\partial \boldsymbol{q}} - f_T(t_{1s})\frac{\partial \rho_s}{\partial \boldsymbol{q}}\right). \quad (4)$$

2.1. Relativistic equations of motion

The spacecraft ephemeris is generated by numerically integrating the equations of motion using the Bulirsh-Stoer method (Press et al. 1996). The equations of motion were represented by the β- and γ-parameterized post-Newtonian (PPN) approximation formulated in the solar system barycentric frame of reference (Moyer 2000). General relativity corresponds to $\beta = \gamma = 1$ which were chosen for this study. Relativistic equations of motion are not necessary to analyze the Pioneer anomalous acceleration as demonstrated by Markwardt (2002). They are more than four orders of magnitude smaller than the anomalous acceleration.

A natural choice for this study is the International Celestial Reference Frame (ICRF) with the SSB as origin. The coordinates of the uplink station, spacecraft and downlink station ($\boldsymbol{r}_1$, $\boldsymbol{r}_2$ and $\boldsymbol{r}_3$) must all be expressed in the same coordinate system. $\boldsymbol{r}_2$ was interpolated from the spacecraft ephemeris and therefore already in the desired frame of reference. The station coordinates had to be transformed from the International Terrestrial Reference Frame (ITRF) to the ICRF and then transformed from the geocentric to barycentric coordinates. The International Earth Rotation and Reference Systems Service (IERS) 2003 convention (McCarthy & Petit 2003) and Moyer (2000) covers these transformations.

The coordinates of the Sun, the planets and the Moon with respect to the SSB were interpolated from the Jet Propulsion Laboratory (JPL) DE405 planetary ephemeris, which uses the ICRF. The time argument of DE405 is TDB (Standish 1998), which was used while integrating the equations of motion.

2.2. Parameter estimation algorithms

The parameters were estimated using an ordinary Bayesian Weighted Least Squares (BWLSQ) algorithm, although I initially used a Kalman filter to check the numerical accuracy and stability of the algorithms. Furthermore, I also ran the software on 64-bit computers with quadruple precision to check for any significant round off errors.

The transformation from Earth fixed to space fixed coordinates was computed using the IERS Conventions (McCarthy & Petit 2003). Also included were antenna corrections (Imbriale 2002), troposphere corrections (Niell 1996), and ionosphere corrections (Moyer 2000). With the exception of the troposphere and ionosphere models, the expected accuracy of the space-fixed position of the antennas is approximately 10 cm. I therefore chose not to estimate any of the parameters related to the station coordinates. The ionosphere correction depends heavily on the solar activity and may contain errors up to tens of meters and is probably the largest source of noise in the processed doppler data.

Even though the spin rate of the Pioneer 10 in principle could be estimated from the Doppler data, the change in the spin rate creates a frequency shift on the order of few mHz as pointed out by Markwardt (2002). Therefore I chose to interpolate a table of Pioneers 10's spin history.

To study the variation of the anomalous acceleration, I implemented a Kalman filter with stochastical variables. The anomalous acceleration was modeled as a first order Markow process with colored noise:

$$p_{k+1} = m(t_{k+1}, t_k)p_k + e_k \quad (5)$$

and

$$m(t_{k+1}, t_k) = \mathrm{e}^{-(t_{k+1}-t_k)/\tau}, \quad (6)$$

where τ is the correlation time. t_{k+1} and t_k are the time-tags of observation number k and $k+1$. A correlation time of zero corresponds to a white noise process while an infinite correlation corresponds to a random walk process. The evolution of the stochastic parameter is dependent on the correlation time and the standard deviation, σ_e, of the noise vector e_k. Some care must be taken when selecting σ_e. A too large value of σ_e allows absorbing all of the doppler-noise into the anomalous acceleration, while a too small value forces the stochastic parameter to remain constant. Guided by the results of PA, $\sigma_e = a_0\tau_e$ was chosen. This preserves short-term structures and the general noise level of the doppler data. The estimate of the anomalous acceleration at a given time t_m is based only on the preceding datapoints, and is therefore not optimal estimates. Hence, after forward processing of the data-sets, the results were smoothed with the Rach-Tung-Striebel (RTS) algorithm (Rauch et al. 1965).

3. Results and discussion

The dataset spans the time-interval from January 1987 to July 1998, which is the same interval analyzed in PA. I report best fit values corresponding to each of the three intervals defined by PA. Interval I spans January 1st 1987 to 17 July 1990, Interval II spans July 17th 1990 to July 12th 1992 and Interval III continues up to July 21st 1998.

The parameters included in the fitting model were the initial SSB position and velocity, a constant anomalous acceleration and instantaneous velocity increments along the Earth-spacecraft line for each maneuver. Because of the Pioneer spin, these maneuvers are only important along the Earth-spacecraft line, and I chose to use the same model as Markwardt (2002) for the maneuvers. PA models the maneuvers as instantaneous velocity increments along the three spacecraft axes. The timing of each maneuver was provided by Slava Turyshev. After each maneuver there are small velocity discontinuities, which arise from fitting the maneuvers to the entire data interval. This is a cause of concern as it indicates that the maneuvers are absorbing unmodeled effects. One possible way to resolve this problem is to determine each maneuver from a limited dataset centered on the corresponding maneuver time. Another possibility is allowing the Pioneer Anomaly to change slowly over time, which makes it possible for the maneuvers to only absorb velocity discontinuities.

To compare my software with those of PA, I fitted the maneuvers using the entire data intervals. My results before systematic errors are given in Table 1 together with the results from JPL's ODP/Sigma and Aerospace Corporation's Compact High Accuracy Satellite Motion Program (CHASMP), which are given by PA. The given uncertainties are only formal calculation errors reported by the fitting program. The different results are most likely caused by how the maneuvers were modeled and especially for Pioneer 11, the a priori magnitude of each maneuver. Setting the a priori velocity increments of each maneuver to zero yielded an initial estimate of $(8.80 \pm 0.5) \times 10^{-8}$ cm/s^2 for

Table 1. The Pioneer anomalous acceleration in units of 10^{-8} cm/s^2. This table displays the results from JPL's orbit determination program, the Aerospace Corporation's CHASMP and and the HELIOSAT program developed by the author at the University of Oslo.

Software	Pioneer 10 (I)	Pioneer 10 (II)	Pioneer 10 (III)	Pioneer 11
ODP/Sigma	8.00 ± 0.01	8.66 ± 0.01	7.84 ± 0.01	8.44 ± 0.04
CHASMP	8.22 ± 0.02	8.89 ± 0.01	7.92 ± 0.01	8.69 ± 0.03
HELIOSAT	7.85 ± 0.02	8.78 ± 0.01	7.75 ± 0.01	8.10 ± 0.01

the Pioneer 11 anomalous acceleration. Taking the a priori magnitudes of each maneuver from analysis with a slowly varying anomalous acceleration, gave results much more similar to those for Pioneer 10. Furthermore, the residuals were now comparable to those for Pioneer 10, i.e. 9.6 mHz compared to 5.8 mHz for Pioneer 10 in interval I. Clearly, I can confirm the presence of unmodelled acceleration acting on the spacecraft. PA have a detailed study of systematics which I will not repeat, thus the results presented in this paper must be compared to their formal estimates of the Pioneer anomaly.

I now return to the velocity discontinuities in the Doppler signal. This indicates either unmodeled forces acting on the spacecraft or unmodeled media corrections affecting the radio signal. To check for time dependent forces I tried to fit the Doppler data to an acceleration of the form

$$a_{\rm P} = a_{\rm P(0)} 2^{-t/\tau}, \tag{7}$$

where τ is 87 years, the half-life of ^{238}Pu. The idea is to test whether heat dissipation from the Radioisotope Thermoelectric Generators (RTG) can explain the data. The radioactive decay of plutonium produces approximately 2 kW of heat, and as little as 65 W, if radiated asymmetrically away from the Sun, would produce the required acceleration. One of the arguments put forth by PA against heat dissipation as the explanation for the Pioneer Anomaly, is the apparent constancy of the anomalous acceleration, although they argue convincingly against asymmetrical heat dissipation on physical grounds too. Scheffer (2003) though argues how the required acceleration can be produced. My analysis of the data show that the χ^2 and the variance remain unchanged for each of the three intervals to within one percent when using the above model for the unmodeled acceleration. To check the constancy of the acceleration over the entire eleven and a half years with data, I merged the three intervals. The boundaries between each of these intervals correspond to changes in the spin-down rate of Pioneer 10. PA assumes the spin-rate change is directly contributing to an anomalous acceleration and suggests the following lever arm model:

$$a_{\rm P}(\ddot{\theta}) = a_{\rm P(0)} - \kappa\,\ddot{\theta}, \tag{8}$$

with $\ddot{\theta}$ being the spin rate change and κ the lever arm length. From this model my base line experimental value for a constant anomalous acceleration is

$$a_{\rm P} = (7.72 \pm 0.01) \times 10^{-8}\ {\rm cm/s^2} \tag{9}$$

with

$$\kappa = (38.4 \pm 0.4)\ {\rm cm}. \tag{10}$$

The corresponding results for ODP/Sigma and CHASMP are $a_{\rm P} = (7.82 \pm 0.01) \times 10^{-8}$ cm/s^2 and $\kappa = (29.2 \pm 0.2)$ cm and $a_{\rm P} = (7.89 \pm 0.02) \times 10^{-8}$ cm/s^2 and $\kappa = (34.7 \pm 0.2)$ cm. The results from ODP/Sigma and CHASMP are computed from a least squares fit of the anomalous acceleration and average spin-down rates in each interval and not directly from a least squares fit to the data set. I found no statistical significant differences between

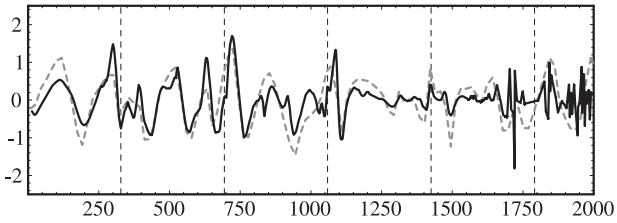

Fig. 1. The variation of the anomalous acceleration of Pioneer 10 in units of 10^{-8} cm/s^2 as function of days since July 12th 1992. The gray dashed line represents the results from a least squares routine with 12 day arcs, while the black line represents the final results from a Kalman filter with stochastical variables. Each vertical dashed line corresponds to conjunctions.

the constant acceleration model and the heat dissipation model, indeed the reduced χ^2 for the heat dissipation model over the 11 year interval is approximately 1 per cent lower than that of the constant acceleration model. A total of

$$P = (61.1 \pm 0.1)\ {\rm W} \tag{11}$$

by January 1st 1987 will explain the Pioneer 10 anomaly. Markwardt (2002) estimated a jerk term, but not with the full data set and without a lever arm parameter. He concluded however that temporal variations of the anomalous acceleration must happen on time scales larger than 70 years. Using Eq. (7) to estimate both $a_{\rm P}(0)$ and τ yields a half life with one standard deviation of

$$\tau = (117 \pm 16)y. \tag{12}$$

Since the anomalous acceleration has significant periodic changes, Eq. (12) probably does represent a meaningful result, but the data do show that heat dissipation can not be excluded as an explanation for the Pioneer anomalous acceleration.

3.1. Variation of the Pioneer anomaly

Still, the heat dissipation model does not remove the velocity discontinuities. I therefore decided to investigate the annual term reported by Turyshev et al. (1999). My first analysis using a Kalman filter with stochastic parameters and a correlation time of 200 days, seemed to confirm the presence of an annual term with a magnitude of

$$\Delta a_{\rm p} \approx 1.5 \times 10^{-8}\ {\rm cm/s^2}. \tag{13}$$

Figure 14 of PA shows 5-day sample averages of the anomalous acceleration of Pioneer 10 from ODP/Sigma using batch sequential filter with a 200-day correlation. But, any changes in the correlation time lead to quite different results with the Kalman filter. I therefore tried another approach. The data set was divided into 12 day long arcs. Each arc determined the anomalous acceleration within each arc without any correlation with the other arcs. The initial conditions and the maneuvers were determined from the entire dataset. Figure 1 shows these results as a gray

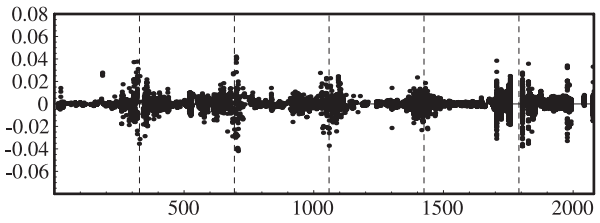

Fig. 2. Doppler residuals for Pioneer 10 using the anomalous acceleration given by Fig. 1. The residuals are given in Hz as function of days since July 12th 1992. Vertical dashed lines correspond to conjunctions.

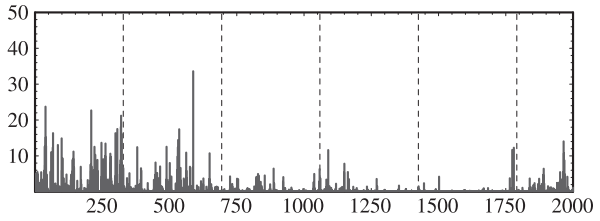

Fig. 3. The Solar Index for the northern hemisphere as a function of days since July 12th 1992. Vertical dashed lines correspond to conjunctions.

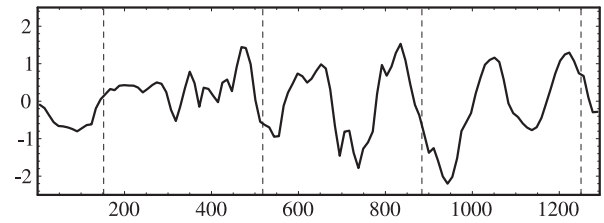

Fig. 4. The variation of the anomalous acceleration of Pioneer 10 in units of 10^{-8} cm/s^2 as function of days since Januray 1st 1987. The black line represents the results from a least squares routine with 12 day arcs. Vertical dashed line corresponds to conjunctions.

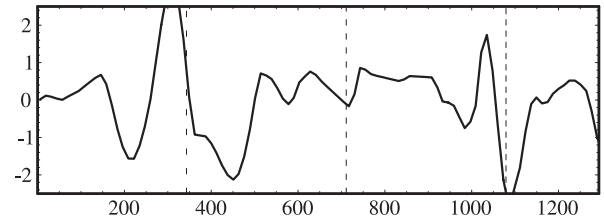

Fig. 5. The variation in the anomalous acceleration of Pioneer 11 in units of 10^{-8} cm/s^2 as function of days since January 1st 1987.

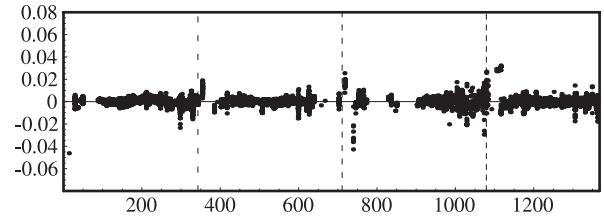

Fig. 6. Doppler residuals for Pioneer 11 using the anomalous acceleration given by Fig. 5. The residuals are given in Hz as function of days since January 1st 1987.

dashed line. The variation of the anomalous acceleration was decreasing until 1996 and then appears to increase again. This corresponds nicely with the previous Solar Cycle, which reached a minimum in 1996, see Fig. 3. It is of interest to consider major solar events, like Coronal Mass Ejections (CME). A typical CME ejects according to the Naval Research Laboratory Solar Physics Branch[2] from 10^{14} g to 10^{17} g of plasma into interplanetary space at speeds ranging from a few hundred km s^{-1} to 2000 km s^{-1} (Burkepile et al. 2004). CMEs may influence the Doppler measurements either through drag on the spacecraft or through plasma delay of the radio transmissions. The light time delay due to electron plasma is to the first order given by

$$\Delta t = 40.3 \frac{TEC}{cf^2}, \tag{14}$$

where TEC is the total electron content, f is the carrier frequency and c is the speed of light. A 50-day half sinusoid with an acceleration amplitude of 1.0×10^{-8} cm/s^2 corresponds to a media correction of approximately half a kilometer. The frequency dependency of the plasma delay means that this effect will be less important for newer deep space spacecraft which usually operate on the X-band. The required electron content for a range correction Δr is

$$TEC = \frac{\Delta r}{40.3} f^2 \approx 8 \times 10^3 \text{ TECU}, \tag{15}$$

where TECU is 10^{16} electrons/m^2. Typical values for Earth's ionosphere are 5 to 50 TECU. To estimate the size of the CME we assume uniform and spherical density distribution. CMEs evolve from a spherical shape into a convex-outward; "pancake" shape (Riley & Crooker 2004). The radius for a spherical shape is given by

$$R_{\rm CME} = \left(\frac{6 n_{\rm e}}{4\pi TEC} \right)^{1/2}, \tag{16}$$

where $n_{\rm e}$ is the total number of electrons and TEC is the required electron content. The given mass range corresponds to a radius range of 1 to 30 solar radii. Relaxation of the uniform density assumption may increase the size estimate significantly if we also assume that the light path passes through the densest part of a CME. Even though CMEs are quite large in angular extent, simulations show that they retain a small dense core (Chané et al. 2006). Furthermore, the effect from CMEs on the light time delay will be largest close to conjunction, since the CMEs are then closer to the Sun when they interfere with the radio transmission. Figure 1 shows variations of the acceleration lasting over an extended period of time, and not at most a few days as would be expected from a CME directed towards Pioneer 10 during conjunction. This may be understood as a result of the a priori assigned accuracy of the anomalous acceleration parameter. To avoid letting the acceleration parameter absorb maneuvers or change the orbit of Pioneer 10 significantly, I had to restrict how much this parameter was allowed to vary from the a priori estimate of the anomalous acceleration. To achieve the required light path correction, the estimation software instead returns a small acceleration lasting a long time. Also, since the orbital inclination of Pioneer 11 is larger than the orbital inclination of Pioneer 10, fewer CMEs is expected to interfere with the radio transmissions. The variation of the anomalous acceleration for Pioneer 10 and 11 during the same interval of time are shown in Figs. 4 and 5 respectively. Especially the results for Pioneer 11 show no clear annual variation of the anomalous acceleration.

The drag acting on a spacecraft due to a CME is

$$a_{\rm CME} = -\kappa_{\rm s} \frac{\rho v^2 A_{\rm s}}{m_{\rm s}}, \tag{17}$$

[2] http://lasco-www.nrl.navy.mil/cmelist.html

where ρ is the density of the CME at the spacecraft, v is the velocity of the CME relative to spacecraft, κ is the effective reflection/absorption/transmission coefficient of the spacecraft for the particles hitting it, A_s is the effective cross-sectional area of the craft, and m_s is its mass. But, only fast and massive CMEs would be able to cause accelerations on the order of 10^{-8} cm/s^2. A 10^{16} g, 2000 km s^{-1} CME which has evolved into a uniform disk with a thickness to radius ratio of 0.1, will give an acceleration of 10^{-8} cm/s^2 if the radius is 2 AU. A similar 500 km s^{-1} CME can not have a radius larger than 0.8 AU. These shock-fronts will pass a spacecraft in a matter of hours and can therefore not be the cause of the variations in the anomalous acceleration.

Clearly, CMEs can have a significant influence on the Doppler measurement through plasma delay of the radio signal. As long as this effect is not removed the spacecraft's orbits will be incorrectly modeled. Any error in the spacecraft's orbits introduces either annual or diurnal (or both) signals in the Doppler residuals. Furthermore, if the spacecraft is tracked over several years, any estimation algorithm forces these terms to be of the same magnitude when minimizing the residuals. PA reported an annual and diurnal signal of 0.1 mm/s at the end 1996. These values are confirmed by my analysis too. Note, however that this annual term is of the order of 0.2×10^{-8} cm/s^2 compared to the 1.6×10^{-8} cm/s^2 oscillatory term reported by Turyshev et al. (1999).

4. Conclusions

A study of the constancy of the Pioneer anomalous acceleration has been presented. Based on the data there is no reason to exclude heat dissipation as the source of the anomaly. Scheffer (2003) argues how such acceleration may be produced and this is not repeated here. The Doppler data cannot be used to separate between a constant acceleration and a slowly decreasing acceleration.

There are significant unmodeled short term effects acting on the spacecraft or on the radio transmissions. The magnitudes of these terms are consistent with expected values of radio plasma delay and the electron content of Coronal Mass Ejections.

Small annual and diurnal terms are understood as an artifact of the maneuver estimation algorithm and unmodeled effects. When the estimation algorithm minimizes the residuals, it returns a slightly incorrect spacecraft trajectory, and the Earth's orbit and rotation appear in the Doppler residuals through the calculated round-trip light times.

Acknowledgements. I would like thank to John D. Anderson and Jet Propulsion Laboratory for letting me stay at JPL as a visiting scientist during 2001. Slava Turyshev and John D. Anderson provided the tracking and spin data used in this study. Their experience made it possible for me to develop a high precision orbit determination program in a relative short time. Finally, I would like to thank Per Helge Anderson for long discussions on statistical estimation algorithms, most of which were not used in this study.

References

Anderson, J. D., Laing, P. A., Lau, E. L., et al. 2002, Phys. Rev. D, 65, 082004
Burkepile, J. T., Hundhausen, A. J., Stanger, A. L., St. Cyr, O. C., & Seiden, J. A. 2004, J. Geophys. Res., 109, A03103
Chané, E., Van der Holst, B., Jacobs, C., Poedts, S., & Kimpe, D. 2006, A&A, 447, 727
Imbriale, W. A. 2002, Large Antennas of the Deep Space Network, Monograph 4, Deep Space Communications and Navigation Series
Markwardt, C. B 2002 [arXiv:gr-qc/0208046]
McCarthy, D. D., & Petit, G. 2003, IERS Conventions (2003), IERS Technical Note, No. 32
Moyer, T. D. 2000, Formulation for Observed and Computed Values of Deep Space Network Data Types for Navigation Monograph 2, Deep Space Communications and Navigation Series
National Geophysical Data Center, http://www.ngdc.noaa.gov/stp/SOLAR/ftpsolarflares.html
Niell, A. E. 1996, J. Geophys. Res., 101, 3227
Press, W. H., Teukolsky, S. A., Vetterling, W. T., & Flannery, B. P. 1996, Numerical Recipes in Fortran 90, 2nd edn. (Cambridge: Cambridge University Press)
Rauch, H. E., Tung, F., & Striebel, C. T. 1965, Maximum likelihood estimates of linear dynamic systems, American Institute of Aeronautics and Astronautics, 3, 1445
Riley, P., & Crooker, N. U. 2004, Kinematic Treatment of Coronal Mass Ejection Evolution in the Solar Wind, ApJ, 600, 1035
Scheffer, L. K. 2003, Phys. Rev. D, 67, 084021
Standish, E. M. 1998, A&A, 336, 381
Turyshev, S. G., Anderson, J. D., Laing, P. A., et al. 1999, The Apparent Anomalous, Weak, Long-Range Acceleration of Pioneer 10 and 11 [arXiv:gr-qc/9903024]